

## Plasmon Resonance Shifts of Au-Coated Au<sub>2</sub>S Nanoshells: Insight into Multicomponent Nanoparticle Growth

R. D. Averitt, D. Sarkar, and N. J. Halas

*Department of Electrical and Computer Engineering, The Rice Quantum Institute and the Center for Nanoscale Science and Technology, Rice University, 6100 South Main, Houston, Texas 77005*

(Received 4 December 1996)

In this Letter we present a coherent description of the optical properties of a unique type of nanoparticle, metal-coated dielectric nanoparticles. These structures occur naturally in the form of Au-coated Au<sub>2</sub>S nanoparticles. During the course of nanoparticle growth, the plasmon-related absorption peak undergoes very large shifts in wavelength, from ~650 to ~900 nm. We show that this plasmon peak shift is purely classical in origin and is determined solely by the relative thickness of the Au shell and the Au<sub>2</sub>S core diameter. This understanding of the optical properties of these nanoparticles is used to elucidate the nanoparticle growth kinetics. [S0031-9007(97)03286-9]

PACS numbers: 61.46.+w, 36.40.Vz, 82.70.Dd

Colloidal gold is, in many ways, the prototypical metallic nanoparticle. Its remarkable properties have been the subject of numerous investigations and applications since before the time of Faraday. In recent years, investigations of gold nanoparticles have increased due to their novel nanoscopic properties and device applications [1–4]. In this Letter, we describe the properties of Au-coated dielectric nanoparticles, or gold nanoshells. This configuration of a dielectric core coated with a metal nanoshell occurs naturally in the growth of Au/Au<sub>2</sub>S nanoparticles. Gold nanoshells possess quite remarkable optical properties that differ dramatically from those of solid gold nanoparticles. During the course of nanoparticle growth, which takes place via reduction in solution, the plasmon absorption peak typically shifts from ~650 to ~900 nm or beyond, depending on reactant concentration. By comparison, the plasmon peak shifts observed in solid gold nanoparticles, via size variation or adsorption of molecular or dielectric species, are negligible (<10 nm) [5]. This unique redshifting of the nanoparticle plasmon resonance to wavelengths in the visible and near infrared regions of the spectrum, a wavelength region of extreme technological interest, may prove to be of tremendous importance for optical applications.

A previous study by Zhou *et al.* established the existence of the Au-coated Au<sub>2</sub>S nanoparticles [6]. However, we conclude that various aspects of their analysis are contradictory to our results. Most importantly, Zhou *et al.* attribute the initial redshift of the Au-coated Au<sub>2</sub>S nanoparticle absorption peak to quantum confinement in the thin Au nanoshell. Our calculations show that quantum confinement (or classically, surface electron scattering) does not result in a redshift of the absorption peak. We show that the reduced mean free path of conduction electrons in the Au shell does result in broadening of the plasmon peak, but this phenomenon does not shift the plasmon resonance. In short, our results show that the plasmon shift is classical in origin, and is determined

by the dimensions and the dielectric properties of the Au<sub>2</sub>S core and the Au shell. In addition, Zhou *et al.* state that at later times in the reaction S<sup>2-</sup> diffuses through the gold shell and reduces the Au<sub>2</sub>S core, resulting in an increase in the shell thickness with the core becoming smaller until the particles become pure gold. This kinetic scenario is unlikely for the following simple reason: S<sup>2-</sup> does not exist in aqueous solution at any pH [7]. This improved understanding of the optical properties of Au nanoshells allows us to probe the growth kinetics of these nanoparticles, where our results indicate that the plasmon peak shift is consistent with a two-stage model of nanoparticle growth where first the Au<sub>2</sub>S core, then the Au shell, grows linearly in time.

ACS reagent grade HAuCl<sub>4</sub> and Na<sub>2</sub>S were obtained from Sigma. Either triply distilled or HPLC grade H<sub>2</sub>O were used for making the aqueous solutions. The typical reaction was started by mixing 1 mM Na<sub>2</sub>S in 2 mM HAuCl<sub>4</sub> with a 1.2:1 volume ratio.

Previous studies have demonstrated that S<sup>2-</sup> is never a dominant aqueous species at any pH [7]. When Na<sub>2</sub>S is mixed with water at pH 7, the S<sup>2-</sup> reacts with the water to give HS<sup>-</sup> and OH<sup>-</sup>. Thus, the initial reactants are AuCl<sub>4</sub><sup>-</sup> and HS<sup>-</sup>. This and simple electrochemical considerations lead us to propose the following reaction for the reduction process leading to the growth of Au-coated Au<sub>2</sub>S nanoparticles:



Au and S are then available for subsequent nucleation and growth. Both Au and Au-coated Au<sub>2</sub>S nanoparticles are grown simultaneously under these reaction conditions. Nanoparticle growth was monitored using a Hitachi U2000 spectrophotometer and the UV-visible spectrum was recorded from 400 to 1050 nm every few minutes. A sequence of UV-vis absorption spectra obtained during a typical reaction is shown in Fig. 1. There are two peaks in each spectrum due to the simultaneous formation

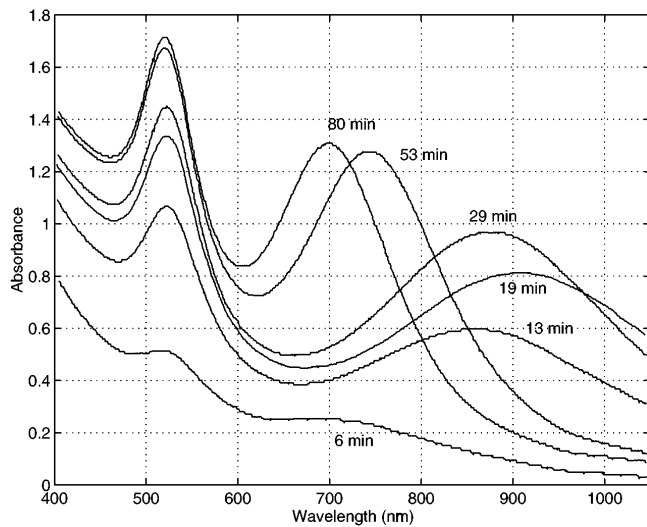


FIG. 1. Evolution of the UV-vis absorption spectrum as the nanoparticle growth proceeds. The peak at  $\sim 520$  nm is due to the plasmon resonance of pure gold colloid. The second peak is due to the plasmon resonance of Au-coated  $\text{Au}_2\text{S}$  nanoparticles. Each spectrum is labeled by the corresponding reaction time.

of solid Au nanoparticles and Au-coated  $\text{Au}_2\text{S}$  nanoparticles. The absorption peak which remains at  $\sim 520$  nm throughout the reaction is due to the plasmon resonance of gold colloid. The second peak is due to Au-coated  $\text{Au}_2\text{S}$  nanoparticles as originally determined by Zhou *et al.* [6]. As the reaction proceeds, this peak first redshifts, and then at later times there is a dramatic blueshift. As the reaction progresses, the FWHM of the Au nanoshell peak narrows from 0.75 to 0.45 eV.

The size distribution of the Au-coated  $\text{Au}_2\text{S}$  nanoparticles was determined from transmission electron microscopy (TEM). A histogram was obtained using the NIH IMAGE program to measure the diameter of each particle [8]. The Au-coated  $\text{Au}_2\text{S}$  nanoparticles have an average diameter of 40 nm at the end of the reaction (with the reaction conditions as described above) and can be described by a Gaussian distribution. The standard deviation ranges from about 10% to 20% in different samples.

It is well established that the optical absorption spectra of alkali and noble metal nanoparticles consist of strong peaks that originate from plasmon excitations. Therefore, we would also expect the optical spectra of metal nanoshells to be plasmonic in origin. We employ a generalized Mie scattering approach [9,10] to calculate the absorption and scattering cross sections of metal nanoshells, using the specific geometry shown in Fig. 2. The core consists of a sphere of radius  $R_c$  with a dielectric constant  $\epsilon_c = 5.4$ . The core dielectric constant was determined by using the calculated band gap for  $\text{Au}_2\text{S}$  [11] and the empirical expression  $\epsilon_c^2 E_g = 77$  where  $\epsilon_c$  is the dielectric constant and  $E_g$  is the band gap [12]. Surrounding this core is a concentric shell for a total nanoparticle radius  $R$ , where values of the experimentally measured bulk permit-

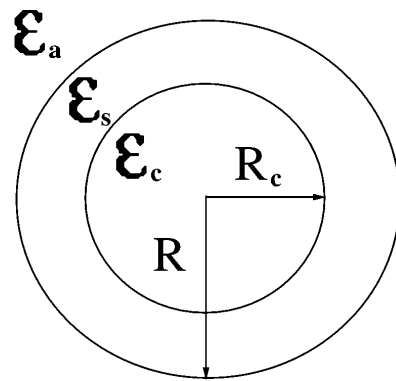


FIG. 2. Nanoshell geometry used in Mie scattering calculations. The  $\text{Au}_2\text{S}$  core has radius  $R_c$  and the total nanoparticle radius is  $R$ . Permittivities are given in text.

tivity  $\epsilon_s(\omega)$ , modified as discussed below, were used [13]. The core-shell system is embedded in an aqueous medium of dielectric constant  $\epsilon_a = 1.78$ .

For a complete description of the plasmon response of metal nanoshells, line broadening mechanisms must also be considered. Since the gold shells of these nanoparticles are thinner than the bulk electron mean free path in gold, a contribution to the dielectric function due to size-dependent electron scattering becomes important. The width of the absorption peak when size-dependent electron scattering becomes important can be described as a modification of the bulk collisional frequency [5],

$$\Gamma = \gamma_{\text{bulk}} + A \times V_F/a, \quad (2)$$

where  $\gamma_{\text{bulk}}$  is the bulk collisional frequency  $V_F$  is the Fermi velocity, and  $a$  is the reduced electron mean free path. For our nanoparticles, we take  $a$  equal to the shell thickness,  $(R - R_c)$ .  $A$  is a parameter which depends upon the geometry and theory used to derive this expression [14]. In the context of simple Drude theory and isotropic scattering,  $A = 1$ . The bulk dielectric function of the gold nanoshells is then modified as follows:

$$\epsilon_s(a, \omega) = \epsilon(\omega)_{\text{exp}} + \frac{\omega_p^2}{\omega^2 + i\omega\gamma_{\text{bulk}}} - \frac{\omega_p^2}{\omega^2 + i\omega\Gamma}. \quad (3)$$

$\epsilon_s(a, \omega)$  is the size-dependent dielectric function where  $\epsilon(\omega)_{\text{exp}}$  is the experimental dielectric function [13], and  $\omega_p$  is the bulk plasmon frequency of gold. Additionally, in any colloidal precipitation process there is a distribution of nanoparticle sizes, leading to inhomogeneous broadening of the absorption spectrum. Although quite often a log-normal distribution describes the size population distribution [15], TEM statistics on Au-coated  $\text{Au}_2\text{S}$  nanoparticles indicate that they can be well described by a Gaussian size distribution with a standard deviation of 10%–20% for the total radius.

By including both size-dependent and inhomogeneous broadening in our Mie calculations, the plasmon peak width narrowing, in addition to the plasmon peak shifts, can be accounted for as nanoparticle growth proceeds. Figure 3 shows how the calculated plasmon peak compares in both peak location and width to the experimentally observed peaks, at six different times during the reaction. In these calculations, the specific values for the core radius  $R_c$  and total radius  $R$  are obtained via our growth model, as discussed below. For the gold shell, we use the size-dependent dielectric function [Eq. (3)]. The pure gold colloidal plasmon resonance is also included in this fit. For each spectrum, only the total particle radius  $R$  was adjusted within experimental uncertainties. A population size distribution of standard deviation  $\sigma = 11\%$  in agreement with our experimentally obtained TEM statistics, was also included. Early in the growth reaction, the peak widths predicted by our model are slightly larger than those experimentally observed. This could be due to the fact that the size distribution is initially narrow and broadens as the reaction proceeds. In fact, if the broadening due to the population size distribution is neglected for the earliest reaction times (while still including size-dependent electron scattering), the agreement with experiment further improves. The pluses in Figs. 3(a) and 3(b) show the results of calculations where the size distribution of nanoparticles is neglected. In general, at all times during the reaction this theoretical approach yields excellent agreement with experiment.

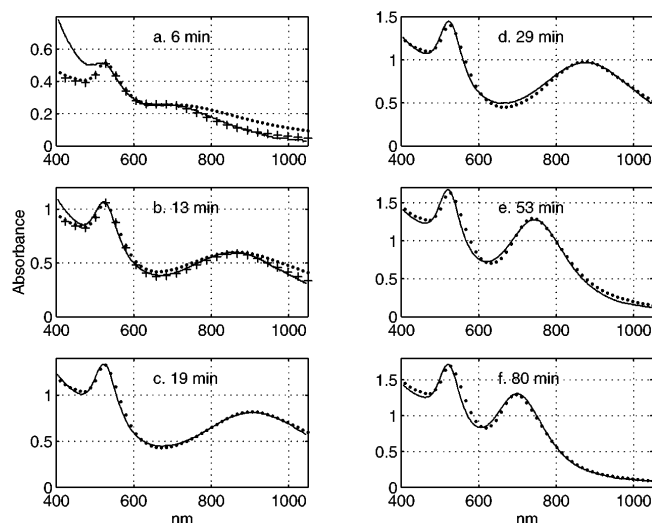


FIG. 3. (a)–(f) Comparison between Mie scattering calculations (dotted line), including the line broadening effects mentioned in text, and experimentally obtained UV-vis spectra (solid line) as nanoparticle growth proceeds. Calculations are obtained using a size distribution with standard deviation  $\sigma = 11\%$ . The + symbols in (a) and (b) are calculations performed with a standard deviation in the size distribution of  $\sigma = 0\%$ . (a)  $R_c = 4.1$  nm,  $R = 5.1$  nm. (b)  $R_c = 8.6$  nm,  $R = 9.9$  nm. (c)  $R_c = 13.1$  nm,  $R = 14.8$  nm. (d)  $R_c = 15.1$  nm,  $R = 17.3$  nm. (e)  $R_c = 15.2$  nm,  $R = 18.8$  nm. (f)  $R_c = 15.2$  nm,  $R = 19.3$  nm.

We have applied this quantitative understanding of the optical properties of metal nanoshells to gain insight into the growth kinetics of Au-coated  $\text{Au}_2\text{S}$  nanoshells. In general, the kinetics of colloid precipitation is quite complex and only specialized cases have been solved analytically. For example, for ideal diffusion limited growth the nanoparticle radius grows according to  $(\text{time})^{1/2}$ , whereas for surface-limited reactions, the particle radius follows a linear growth law [16,17]. During the initial  $\sim 20$  min of Au-coated  $\text{Au}_2\text{S}$  nanoparticle growth, we assume that the core radius grows linearly in time. This model for  $\text{Au}_2\text{S}$  nanoparticle core growth is shown in Fig. 4(a). After  $\sim 20$  min, and consistent with reactant depletion, the core growth stops, the core radius remains constant at  $\sim 15$  nm, and the Au nanoshell increases in thickness. Comparison of plasmon shifts calculated for the nanoparticle geometry of Fig. 2 using this model for the core growth permits us to theoretically predict the Au nanoshell thickness as a function of time during nanoparticle growth. We also employ a constraint obtained from TEM analysis: the nanoparticle diameter must asymptotically approach the observed value of 40 nm. Figure 4(b) shows the calculated plasmon peak position vs time corresponding to the core radii of Fig. 4(a). The experimental plasmon peak location is also plotted in Fig. 4(b),

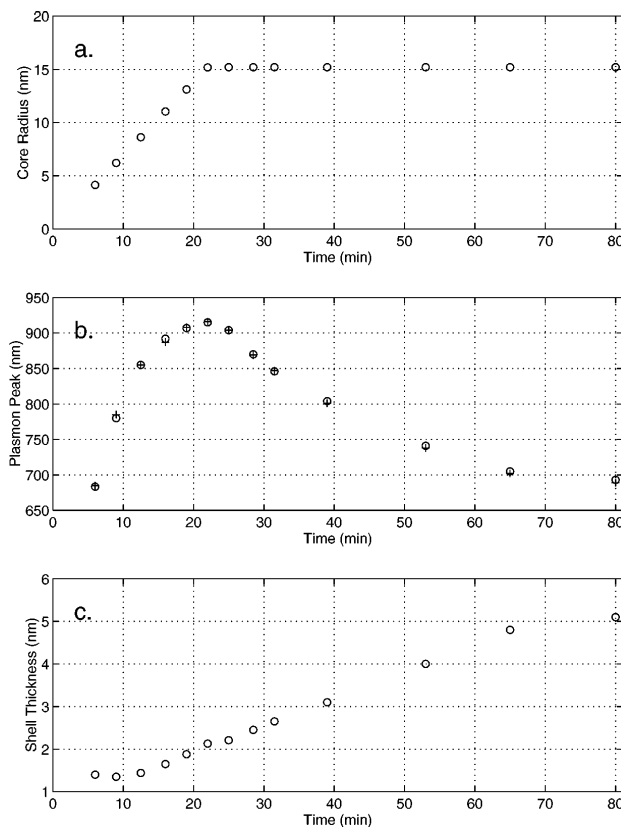


FIG. 4. (a) Postulated growth for the  $\text{Au}_2\text{S}$  core. (b) Calculated (o) and experimental (+) plasmon peaks for the Au nanoshells as nanoparticle growth proceeds. (c) Calculated Au nanoshell thicknesses.

indicating that experimental observations and theoretical calculations agree for all times during nanoparticle growth. To obtain this agreement, only the relative shell thickness,  $R - R_c$ , is adjusted. The shell thickness obtained through this procedure is plotted in Fig. 4(c). Notice that the quantitative agreement between the experimental and theoretical plasmon shifts shown in Fig. 4(b) is consistent with a nanoparticle shell thickness that increases linearly with time. This result strongly reinforces a model of two-stage surface-limited growth, where first the core and then the nanoshell radius grow linearly with time.

In conclusion, we have explained the optical properties of Au-coated Au<sub>2</sub>S nanoparticles, based on generalized Mie scattering calculations for the nanoshell geometry. The large plasmon peak shifts observed in this unique dielectric core-metal nanoshell system are classical in origin and dependent upon both the radius of the Au<sub>2</sub>S nanoparticle core and the metal nanoshell thickness. Our results also show that the plasmon peak width is due to the reduced mean free path of the conduction electrons in the Au shell, as well as the size distribution of nanoparticles. The correlation between the optical properties and a linear growth model for the nanoparticle core permits us to invoke a two-stage linear growth scenario for both the core and the shell of this unique nanoparticle.

We would like to thank T. Randall Lee for discussions regarding the chemistry and Ove Jepsen for band structure calculations on Au<sub>2</sub>S. We would additionally like to thank the Robert A. Welch Foundation and the Texas Advanced Technology Program. N.J.H. is the recipient of an NSF Young Investigator (NYI) award.

- [1] R. P. Andres, J. D. Bielefeld, J. I. Henderson, D. B. Janes, V. R. Kolagunta, C. P. Kubiak, W. J. Mahoney, and R. G. Osifchin, *Science* **273**, 1690 (1996).
- [2] R. G. Freeman *et al.*, *Science* **267**, 1629 (1995).
- [3] P. C. Ohara, D. V. Leff, J. R. Heath, and W. M. Gelbart, *Phys. Rev. Lett.* **75**, 3466 (1995).
- [4] R. P. Andres, T. Bein, M. Dorogi, S. Feng, J. I. Henderson, C. P. Kubiak, W. Mahoney, R. G. Osifchin, and R. Reifengerger, *Science* **272**, 1323 (1996).
- [5] U. Kreibig and M. Vollmer, *Optical Properties of Metal Clusters* (Springer, Berlin, 1995).
- [6] H. S. Zhou, I. Honma, H. Komiyama, and J. W. Haus, *Phys. Rev. B* **50**, 12 052 (1994).
- [7] M. A. A. Schoonen and H. L. Barnes, *Geochim. Cosmochim. Acta* **52**, 649 (1988).
- [8] The size distribution was determined using the public domain NIH IMAGE program on a Macintosh PowerPC. It is available from the Internet via anonymous FTP from [zippy.nimh.nih.gov](http://zippy.nimh.nih.gov).
- [9] D. Sarkar, Ph.D. thesis, Rice University, 1996.
- [10] D. Sarkar and N. J. Halas, *Phys. Rev. E* (to be published).
- [11] O. Jepsen, Au<sub>2</sub>S is a direct band gap semiconductor with  $E_g$  in the range from 1.3 to 2.6 eV (private communication).
- [12] J. I. Pankove, *Optical Processes in Semiconductors* (Dover, New York, 1975).
- [13] P. B. Johnson and R. W. Christy, *Phys. Rev. B* **6**, 4370 (1972).
- [14] U. Kreibig and L. Genzel, *Surf. Sci.* **156**, 678 (1985).
- [15] C. G. Granqvist and R. A. Buhrman, *J. Appl. Phys.* **47**, 2200 (1976).
- [16] A. E. Nielsen, *Kinetics of Precipitation* (Macmillan, New York, 1964).
- [17] J. W. Mullin, *Crystallization* (Butterworth-Heinemann, Oxford, 1993).